# Continuum Radiative Flux from Nonisothermal Nongray Atomic Gases

H. F. NELSON* AND A. L. CROSBIE†
*University of Missouri–Rolla, Rolla, Mo.*

**The continuum radiative flux from a nonisothermal stagnation shock layer composed of an atomic gas is the subject of this numerical study in which the fluid dynamics and the radiation are assumed to be uncoupled. Consequently, the temperature profile, which is taken to vary linearly through the shock layer, is unperturbed by the radiation. The importance of the ionization edge location and the influence of various spectral shapes of the bound-free radiative cross sections are emphasized. The results are derived by considering ground to free state radiative transitions. The principal of superposition extends the results to multiple electronic state atomic gases.**

## Nomenclature

$B$ = $(1 - \theta_o)$, Eq. (21)
$D(t)$ = Debye function
$e_{b\nu}$ = Planck function
$E_m(t)$ = exponential integral of order $m$
$F(t)$ = radiative flux
$\bar{F}$ = $F(t)/\sigma T_r^4$
$h$ = Planck's constant
$k$ = Boltzmann's constant
$L$ = physical thickness of shock layer
$M$ = number of excited electronic states
$n$ = exponent giving frequency dependence of $\alpha(\nu)$
$N_i$ = number density of $i$th electronic state
$\mathrm{sgn}(t)$ = indicator function, 1 for $t > 0$, $-1$ for $t < 0$
$S_i$ = absorption cross section
$t$ = dummy variable
$T$ = temperature
$T_r$ = reference temperature
$x$ = distance into shock layer
$\bar{x}$ = $x/L$
$\alpha(\nu)$ = spectral variation of $\kappa_\nu(x)$, Eq. (7)
$\beta(x)$ = distance variation of $\kappa_\nu(x)$
$\epsilon_\nu$ = spectral emittance
$\theta$ = $T/T_r$
$\kappa_\nu(x)$ = absorption coefficient
$\nu$ = frequency
$\xi$ = optical depth, Eq. (11a)
$\bar{\nu}$ = $h\nu/kT_r$
$\sigma$ = Stefan-Boltzmann constant
$\tau$ = optical thickness, Eq. (11b)
$\tau_\nu$ = optical depth at frequency $\nu$, Eq. (3a)
$\tau_{o\nu}$ = optical thickness of shock layer at frequency $\nu$, Eq. (3b)

***Subscripts***

0 = evaluated at $\bar{x} = 0$
$i$ = electronic state $i = 0$ (ground), $i = 1$ (first excited) etc.

## I. Introduction

LATELY, the prediction of the radiative heating of a blunt body has received considerable attention.[1,2] The shock layer temperature distribution and the radiative characteristics of the shock layer plasma are important factors which influence radiative heating. Most analyses assume an isothermal shock layer[3–6] or a step model absorption coefficient.[7–9] The complexity of the problem precludes precise treatment of every feature of the flow and radiative fields.

Mandell[10,11] and Mandell and Cess[12] investigated radiative transfer in nonisothermal hydrogen plasmas under the conditions of 1) radiative equilibrium, 2) pure radiation with constant heat generation, 3) simultaneous conduction and radiation, and 4) interaction of convection, conduction, and radiation. They considered both continuum and line radiation, assumed the Planck function to be a linear function of temperature, and used the exponential approximation. Their results indicate that line radiation is important only for optically thin plasmas.

The motivation for the present study is to develop an understanding of the coupling of nongray-nonisothermal radiation. As a means of gaining this understanding, the radiative flux from an nonisothermal shock layer has been considered; however, the analysis is not restricted to this physical situation. The radiating plasma consists of an atomic gas. The effects of various gases can be deduced by changing the ionization potential, that is, by changing the ionization edges to match the particular atomic gas of interest in contrast to previous work which usually considered specific gases.

In this study, the following is assumed: 1) local thermodynamic and chemical equilibrium, 2) one-dimensional, radiative energy transport, 3) radiation emitted from the body is negligible, and 4) precursor effects are negligible. Line radiation (bound-bound) and the influence of stimulated emission are not considered.

The actual temperature profile in the shock layer is determined from the coupled conservation equations. Because the object of this study is to investigate nongray-nonisothermal radiation, the fluid dynamics and radiation are uncoupled by assuming a linear temperature profile in the shock layer

$$T/T_r = \theta(\bar{x}) = \theta_o + (1 - \theta_o)\bar{x} \tag{1}$$

This temperature distribution represents the actual temperature profile more accurately than the isothermal approximation which has been used in many other investigations. The shock wave is located at $\bar{x} = 1$ and the body at $\bar{x} = 0$. The reference temperature, $T_r$, is given by the Rankine-Hugoniot equations, and $\theta_o$ is the nondimensional temperature at $\bar{x} = 0$ which is determined by the vehicle's ablating properties. Figure 1 describes the geometry.

The radiation model has been simplified by assuming a hydrogenic gas and considering only continuum (bound-free)

Presented as Paper 70-837 at the AIAA 5th Thermophysics Conference, Los Angeles, Calif., June 29–July 1, 1970; submitted August 5, 1970; revision received May 5, 1971.

Index category: Radiation and Radiative Heat Transfer.

* Assistant Professor, Thermal Radiative Transfer Group Department of Mechanical and Aerospace Engineering. Member AIAA.

† Assistant Professor, Thermal Radiative Transfer Group, Department of Mechanical and Aerospace Engineering.

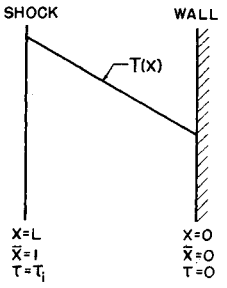


**Fig. 1 Physical model.**

radiative processes. The model can be made to represent various atomic gases by changing the ionization edge location and by changing the spectral form of the absorption coefficient.

## II. Governing Equations and Solutions

The local radiative flux can be written as[13]

$$F(x) = 2\int_0^\infty \int_0^{\tau_{o\nu}} e_{b\nu}(t)\,\mathrm{sgn}(\tau_\nu - t)E_2(|\tau_\nu - t|)dtd\nu \quad (2)$$

where the spectral optical depth and optical thickness are defined as

$$\tau_\nu = \int_0^x \kappa_\nu(x')dx' \quad (3a)$$

and

$$\tau_{o\nu} = \int_0^L \kappa_\nu(x')dx' \quad (3b)$$

The continuum absorption coefficient for a $M + 1$ level hydrogenic gas is given by[14]

$$\kappa_\nu(x) = \sum_{k=0}^{M} \beta_k(x)\alpha_k(\nu) \quad 0 < \nu < \infty \quad (4)$$

where the frequency variation of the $i$th excited state is

$$\begin{aligned} \alpha_i(\nu) &= 0 \qquad \nu < \nu_i \\ \alpha_i(\nu) &= (\nu_i/\nu)^n \quad \nu > \nu_i \end{aligned} \quad (5)$$

The ground state corresponds to $i = 0$, while the first excited state corresponds to $i = 1$. The classical spectral shape of $\alpha(\nu)$ corresponds to $n = 3$; however, many atomic gases have absorption coefficients with spectral variations corresponding to $n$ different than three.[15,16] These differences are accounted for in this study by allowing $n$ to take on different values. Because the $i$th excited state does not influence the absorption coefficient for frequencies less than $\nu_i$, the absorption coefficient for the spectral region, $\nu_i \leq \nu < \nu_{i-1}$, can be written as

$$\kappa_\nu(x) = \sum_{k=i}^{M} \beta_k(x)\alpha_k(\nu) \quad (6)$$

where $\nu_{-1}$ is defined as infinity.

Often the $i$th excited state influences the absorption coefficient only in the spectral interval $\nu_i \leq \nu < \nu_{i-1}$, i.e.,

$$\beta_{i-1}(x)\alpha_{i-1}(\nu_{i-1}) \gg \sum_{k=i}^{M} \beta_k(x)\alpha_k(\nu_{i-1})$$

Mathematically, this approximation can be represented by

$$\kappa_\nu = \beta_i(x)\alpha_i(\nu) \qquad \nu_i \leq \nu < \nu_{i-1} \quad (7)$$

Employing this approximation, the radiative flux becomes

$$F = \sum_{i=0}^{M} F_i \quad (8)$$

where $F_i$ is the flux from the $i$th excited state

$$F_i = 2\int_{\nu_i}^{\nu_{i-1}} \int_0^{\tau_{o\nu}} e_{b\nu}(t)\,\mathrm{sgn}(\tau_\nu - t)E_2(|\tau_\nu - t|)dtd\nu \quad (9)$$

Because the absorption coefficient is a separable function of position and frequency, the radiative flux becomes

$$F_i(\xi_i) = 2\int_{\nu_i}^{\nu_{i-1}} \int_0^{\tau_i} e_{b\nu}(t)\,\mathrm{sgn}(\xi_i - t)\alpha_i(\nu) \times E_2[\alpha_i(\nu)|\xi_i - t|]dtd\nu \quad (10)$$

where the optical depth and thickness of the $i$th excited state are

$$\xi_i = \int_0^x \beta_i(x')dx' \quad (11a)$$

and

$$\tau_i = \int_0^L \beta_i(x')dx' \quad (11b)$$

When

$$2\int_{\nu_{i-1}}^{\infty} \int_0^{\tau_i} e_{b\nu}(t)\,\mathrm{sgn}(\xi_i - t)\alpha_i(\nu)E_2[\alpha_i(\nu)|\xi_i - t|]dtd\nu \ll 2\int_{\nu_i}^{\nu_{i-1}} \int_0^{\tau_i} e_{b\nu}(t)\,\mathrm{sgn}(\xi_i - t)\alpha_i(\nu)E_2[\alpha_i(\nu)|\xi_i - t|]dtd\nu \quad (12)$$

The radiative flux becomes

$$F_i(\xi_i) = 2\int_{\nu_i}^{\infty} \int_0^{\tau_i} e_{b\nu}(t)\,\mathrm{sgn}(\xi_i - t)\alpha_i(\nu) \times E_2[\alpha_i(\nu)|\xi_i - t|]dtd\nu \quad (13)$$

Thus with the approximations, Eqs. (7) and (12), the continuum radiative flux from an excited state is equivalent to the continuum radiative flux from the ground state. Evaluating Eq. (13) for appropriate values of $\nu_i$ and $\tau_i$ and superimposing the solutions via Eq. (8) allows one to calculate the radiation from several bound-free transitions. The validity of the approximations, Eqs. (7) and (12), depends on $n$, $\bar{\nu}_i$, and $\beta_i$,‡ which are properties of the radiating atoms. In general, as $n$, $\bar{\nu}_{i-1} - \bar{\nu}_i$, and $\beta_{i-1}\alpha_{i-1}(\bar{\nu}_{i-1})/[\beta_i\alpha_i(\bar{\nu}_{i-1})]$ are increased, the accuracy of Eq. (13) increases.

By employing the nondimensional frequency ($\bar{\nu} = h\nu/kT_r$) the dimensionless radiative fluxes leaving the shock layer can be written as

$$\bar{F}_i(0) = \frac{F_i(0)}{\sigma T_r^4} = \frac{-30}{\pi^4}\int_{\bar{\nu}_i}^{\infty} \int_0^{\tau_i} \frac{\bar{\nu}^3\alpha_i(\bar{\nu})E_2[\alpha_i(\bar{\nu})t]dtd\bar{\nu}}{\exp[\bar{\nu}/\theta(t)] - 1} \quad (14a)$$

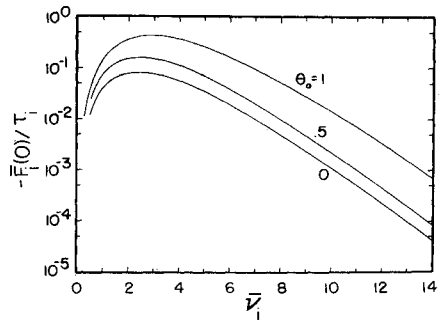


**Fig. 2 Optically thin solution for $n = 3$.**

‡ In this paper, $\beta_i(x)$ is taken to be constant. In general, it is a function of the composition of the plasma.

and

$$\bar{F}_i(\tau_i) = \frac{F_i(\tau_i)}{\sigma T_r^4} = \frac{30}{\pi^4}\int_{\bar{\nu}_i}^{\infty}\int_0^{\tau_i}\frac{\bar{\nu}^3\alpha_i(\bar{\nu})E_2[\alpha_i(\bar{\nu})t]dtd\bar{\nu}}{\exp[\bar{\nu}/\theta(\tau_i - t)] - 1} \quad (14b)$$

### 1. Optically Thin Solution

When the optical thickness becomes small ($\tau_i \to 0$), the radiative flux becomes

$$\bar{F}_i(0) = -\bar{F}_i(\tau_i) = \frac{-30}{\pi^4}\tau_i\int_{\bar{\nu}_i}^{\infty}\int_0^1\frac{\bar{\nu}^3\alpha_i(\bar{\nu})d\bar{x}d\bar{\nu}}{\exp[\bar{\nu}/\theta(\bar{x})] - 1} \quad (15)$$

The spacial integral is evaluated first by changing variables [$y = \theta(\bar{x})$ and $dy = (1 - \theta_o)d\bar{x}$] and then breaking the integral into two parts. Thus, when $\theta_o < 1$, the optically thin flux becomes

$$\bar{F}_i(0) = \frac{-30\tau_i}{(1-\theta_o)\pi^4}\int_{\bar{\nu}_i}^{\infty}\bar{\nu}^3\alpha_i(\bar{\nu})\left[\sum_{m=1}^{\infty}E_2(m\bar{\nu})\right]d\bar{\nu} + \frac{30\tau_i\theta_o}{(1-\theta_o)\pi^4}\int_{\bar{\nu}_i}^{\infty}\bar{\nu}^3\alpha_i(\bar{\nu})\left[\sum_{m=1}^{\infty}E_2(m\bar{\nu}/\theta_o)\right]d\bar{\nu} \quad (16)$$

For the special case of $n = 3$, the flux can be written as

$$\bar{F}_i(0) = \frac{-30\tau_i}{(1-\theta_o)\pi^4}\bar{\nu}_i^3\sum_{m=1}^{\infty}\frac{1}{m}E_3(m\bar{\nu}_i) + \frac{30\tau_i}{(1-\theta_o)\pi^4}\theta_o^2\bar{\nu}_i^3\sum_{m=1}^{\infty}\frac{1}{m}E_3(m\bar{\nu}_i/\theta_o) \quad (17)$$

The optically thin solution for $n = 3$ is presented graphically in Fig. 2. Numerical results have shown that the second term in Eq. (17) can be neglected when $\theta_o \leq 0.5$ or that $(1 - \theta_o)\bar{F}_i(0)/\tau_i$ is independent of $\theta_o$ for $\theta_o \leq 0.5$.

### 2. Optically Thick Solution

When the optical thickness becomes large ($\tau_i \to \infty$), the radiative fluxes leaving the layer are given by

$$\bar{F}_i(0) = -\theta_0^4[1 - D(\bar{\nu}_i/\theta_0)] \quad (18a)$$

$$\bar{F}_i(\tau_i) = 1 - D(\bar{\nu}_i) \quad (18b)$$

where $D(\bar{\nu}_i)$ is the Debye function

$$D(z) = \frac{15}{\pi^4}\int_0^z\frac{x^3}{\exp(x) - 1}dx \quad (19)$$

In this limit, the plasma acts like an opaque solid with surface emittance: $\epsilon_\nu = 0$ for $0 < \bar{\nu} < \bar{\nu}_i$ and $\epsilon_\nu = 1$ for $\bar{\nu} \geq \bar{\nu}_i$.

### 3. Gray solution

The gray situation corresponds to $\bar{\nu}_o = 0$ and $n = 0$. In this case, the integration over frequency can be evaluated analytically, and the flux is given by

$$\bar{F}_0(0) = -2\int_0^{\tau_o}\theta^4(t)E_2(t)dt \quad (20)$$

By substituting the linear temperature distribution and integrating, one obtains

$$\bar{F}_0(0) = -2\left\{\tfrac{1}{2} - E_3(\tau_0) + \frac{4B}{\tau_0}[\tfrac{1}{3} - E_4(\tau_0)] + \frac{12B^2}{\tau_o^2}[\tfrac{1}{4} - E_5(\tau_o)] + \frac{24B^3}{\tau_o^3}[\tfrac{1}{5} - E_6(\tau_o)] + \frac{24B^4}{\tau_o^4}[\tfrac{1}{6} - E_7(\tau_o)] - 2B + 3B^2 - 2B^3 + \tfrac{1}{2}B^4 - (4B^2 - 4B^3 + \tfrac{4}{3}B^4)/\tau_o - (6B^3 - 3B^4)/\tau_o^2 - \tfrac{24}{5}B^4/\tau_o^3\right\} \quad (21)$$

where $B = 1 - \theta_o$. In the optically thin limit ($\tau_o \to 0$), this expression becomes

$$\bar{F}_0(0) = -2\tau_0[1 - 2B + 2B^2 - 3B^3 + \tfrac{1}{5}B^4] \quad (22)$$

### 4. Isothermal Solution

When the layer is isothermal ($\theta_o = 1$), the spacial integration can be carried out analytically. Thus, the flux leaving the isothermal layer is

$$\bar{F}_i(0) = \frac{-30}{\pi^4}\int_{\bar{\nu}_i}^{\infty}\frac{\bar{\nu}^3}{\exp(\bar{\nu}) - 1}\{\tfrac{1}{2} - E_3[\alpha_i(\bar{\nu})\tau_i]\}d\bar{\nu} \quad (23)$$

If $n = 0$, Eq. (23) can be integrated analytically to give

$$\bar{F}_i(0) = -[1 - 2E_3(\tau_i)][1 - D(\bar{\nu}_i)] \quad (24)$$

In the optically thick limit $\tau_0 \to \infty$, the flux becomes independent of $n$. It depends only on the cutoff frequency $\bar{\nu}_i$

$$\bar{F}_i(0) = -[1 - D(\bar{\nu}_i)] \quad (25)$$

The flux becomes sensitive to the form of the absorption coefficient in the thin limit ($\tau_i \to 0$)

$$\bar{F}_i(0) = \frac{-30}{\pi^4}\tau_i\bar{\nu}_i^n\int_{\bar{\nu}_i}^{\infty}\frac{\bar{\nu}^{3-n}}{\exp(\bar{\nu}) - 1}d\bar{\nu} \quad (26)$$

When $n = 0$, the expression becomes

$$\bar{F}_i(0) = -2\tau_i[1 - D(\bar{\nu}_i)] \quad (27)$$

When $n = 3$, the optically thin flux is

$$\bar{F}_i(0) = \frac{30}{\pi^4}\bar{\nu}_i^3\ln[1 - \exp(-\bar{\nu}_i)]\tau_i \quad (28)$$

The general expression for the radiative flux from an optically thin plasma is

$$\bar{F}_i(0) = \frac{-30}{\pi^4}\bar{\nu}_i^n\tau_i\sum_{k=1}^{\infty}e^{-k\bar{\nu}_i}\left[\frac{\bar{\nu}_i^{3-n}}{k} + \frac{(3-n)\bar{\nu}_i^{2-n}}{k^2} + \frac{(3-n)(2-n)\bar{\nu}_i^{1-n}}{k^3} + \frac{(3-n)(2-n)(1-n)}{k^4}\right] \quad (29)$$

### 5. Numerical Solution

The radiative flux as given by Eq. (14) is evaluated by double numerical integration. The frequency integration is performed using Simpson's rule with a fixed step of $\Delta\bar{\nu} = 0.1$ and is terminated at $\bar{\nu} = 20$ for $\bar{\nu}_i \leq 7$ and at $\bar{\nu} = 2.5\bar{\nu}_i$ for $\bar{\nu}_i > 7$. The spacial integration also uses Simpson's rule, but the step size increases with optical depth. The accuracy of the numerical integration is checked by changing the step sizes and comparing the results with the limiting solutions.

## III. Results

The influence of the shape of the absorption coefficient ($n$) and the effect of different ionization edges ($\bar{\nu}_i$) on the radiative flux to the body for several linear temperature profiles ($\theta_o$) can be examined first. After various solutions have been investigated, an application of the results can be considered.

### 1. Influence of $n$

Figure 3 shows the normalized flux $\bar{F}_i(0)$ as a function of optical thickness for several values of $\theta_0$. The absorption coefficient parameters are $\bar{\nu}_i = 2$ and $n = 3$. Figure 4 shows the radiative flux for several values of $n$, for $\theta_o = 1.0$ and 0.5, and $\bar{\nu}_i = 2$.

#### *a. Isothermal*

As the optical thickness at the ionization edge ($\tau_i$) increases from zero for the isothermal cases ($\theta_o = 1$) shown in Figs. 3

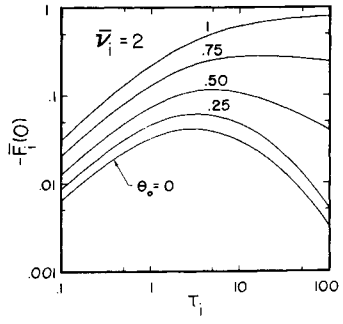


**Fig. 3 Comparison of $\bar{F}_i$ (0) as a function of $\tau_i$ for $n = 3$.**

and 4, $\bar{F}_i(0)$ increases because emission is more important than absorption. As $\tau_i$ continues to increase, absorption begins to become important. As $\tau_i$ becomes very large, the flux approaches its optically thick limit and does not increase for further increases of $\tau_i$.

The influence of $n$ is shown in Fig. 4 for the isothermal case. As one would expect, the value of $\tau_i$ at which the flux reaches its thick limit is dependent upon the value of $n$. For $n = 0$ the optically thick limit is reached at $\tau_i \simeq 3$; whereas, for $n = 3$, it occurs at about $\tau_i \simeq 100$. This occurs because at values of $\bar{\nu}$ greater than the ionization edge, the optical thickness of the $n = 3$ case is much less than the $n = 0$ case, and in turn radiation that is emitted much deeper in the plasma can reach the boundary.

### b. *Nonisothermal*

The influence of the temperature profile is quite strong as can be seen from Figs. 3 and 4. For the nonisothermal cases ($\theta_o \neq 1$), as $\tau_i$ increases from zero, the flux increases because emission is more important than absorption. As $\tau_i$ increases further, absorption becomes important and the flux reaches a maximum and then decreases toward its optically thick limit. For large $\tau_i$, the flux emitted in the high temperature region is strongly attenuated and only that portion emitted in the cool region near the boundary reaches the surface. In the optically thick limit, the radiation which reaches the body behaves as if it were emitted from an opaque plasma at the surface temperature. The absorption coefficient at each frequency beyond $\bar{\nu}_i$ increases as $n$ decreases; therefore, the value of $\tau_i$ at which the maximum flux and the optically thick limit occur decreases.

## 2. Influence of $\bar{\nu}_i$

Figures 5, 6, and 7 show the flux as a function of the ionization edge cutoff for several values of optical thickness for the $n = 3$ absorption coefficient. Figure 5 gives results for the isothermal case, Fig. 6 for the case $\theta_o = 0.5$, and Fig. 7 for the case $\theta_o = 0$.

### a. *Isothermal*

Inspection of Eq. (24) reveals that the radiative flux decreases as $\bar{\nu}_i$ increases for $n = 0$; however, inspection of Fig. 5 for $n = 3$ reveals that the flux first increases and then decreases as $\bar{\nu}_i$ increases. This behavior can be explained by examining the spectral variation of $\alpha_i(\nu)$. The slope of $\alpha_i(\bar{\nu})$ at $\bar{\nu}_i$ is $-n/\bar{\nu}_i$. As $\bar{\nu}_i$ approaches zero, the slope approaches $-\infty$ for $n$ greater than zero; consequently, the entire flux contribution occurs near $\bar{\nu}_i$. As $\bar{\nu}_i$ becomes large, the slope approaches zero and $\alpha_i(\bar{\nu})$ behaves like the $n = 0$ case.

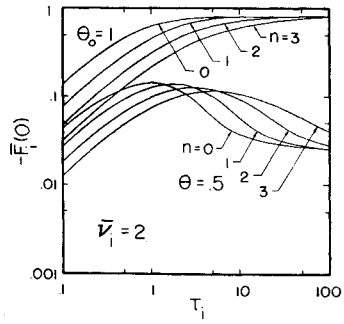


**Fig. 4 Comparison of $\bar{F}_i$ (0) as a function of $\tau_i$ for four values of $n$ and two temperature profiles.**

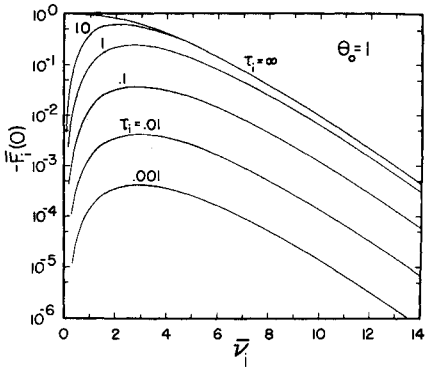


**Fig. 5 Isothermal case; $\bar{F}_i$ (0) as a function of $\bar{\nu}_i$ for various values of $\tau_i$ with $n = 3$.**

Radiation can be transmitted only very near the ionization edge for small $\bar{\nu}_i$; consequently, the flux is very small. The flux increases as $\bar{\nu}_i$ increases not only because the spectral region in which the radiation can be transmitted increases but also because the Planck function in the region near $\bar{\nu}_i$ increases. The flux reaches a maximum and begins to decrease as $\bar{\nu}_i$ increases beyond about three because the radiation is limited to that in the tail of the Planck function.

The value of $\bar{\nu}_i$, at which the flux reaches its optically thick limit, is a function of optical thickness. For an optical thickness less than unity, the flux never becomes optically thick for cutoff values of interest. As the optical thickness increases from unity, the optically thick limit is reached at successively smaller values of the ionization edge frequency.

### b. *Nonisothermal*

For nonisothermal plasmas, the distribution of flux with $\bar{\nu}_i$ at constant values of $\tau_i$ becomes much more complicated. For small optical thickness, the flux behaves like the isothermal case; however, as $\tau_i$ increases beyond unity for values of $\bar{\nu}_i$ beyond the flux maximum, the flux begins to decrease toward the optically thick limit. The reasons for this behavior are that as $\tau_i$ increases, the radiation reaching the boundary is reduced because it is 1) emitted in progressively cooler regions of the plasma, thereby decreasing the value of the source function, 2) influenced by self-absorption, and 3) progressively picks up less and less energy from the source

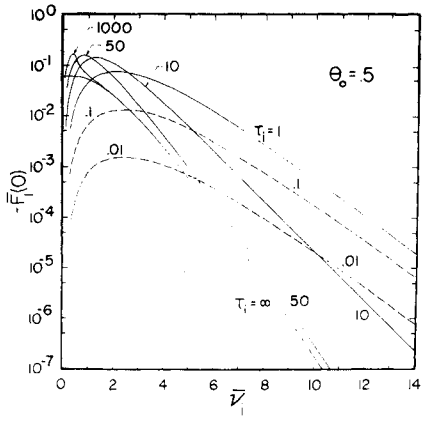


**Fig. 6 Nonisothermal case; $\bar{F}_i$ (0) as a function of $\bar{\nu}_i$ for various values of $\tau_i$ with $n = 3$.**

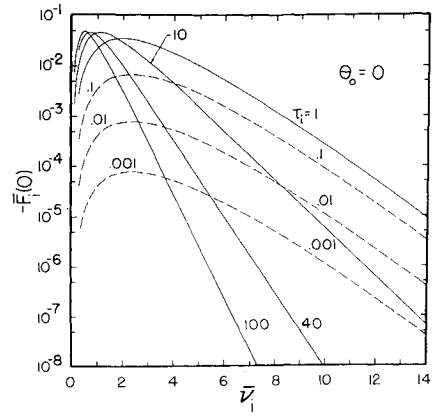


**Fig. 7 Nonisothermal case; $\bar{F}_i$ (0) as a function of $\bar{\nu}_i$ for various values of $\tau_i$ with $n = 3$.**

function as the cutoff frequency increases. Thus, the combined effect of self-absorption and nonconstant temperatures profiles causes the optically thick limit to be approached from above; whereas, in the isothermal case only the self-absorption effect exists, and the optically thick limit is approached from below. Figure 7 shows the $\theta_o = 0$ case. This case shows the same general trends as that of Fig. 6; however, the numerical values are different especially for large $\tau_i$. In the thick limit, the plasma near the boundary will appear to be an opaque gas at zero temperature.

### 3. Precursor Flux

The radiative flux that is lost in front of the shock wave, $\bar{F}_i(\tau_i)$, is shown in Fig. 8 for $\bar{\nu}_i = 2$ as a function of $\tau_i$ for several temperature profiles. This case behaves much like the isothermal cases analyzed previously. The flux increases as $\tau_i$ increases until self-absorption becomes important and then it approaches its optically thick limit which depends only on the position of the ionization edge. In the optically thick limit, the only radiation that can be lost is that which is emitted very near the shock wave. This radiation is essentially emitted from an isothermal plasma at the reference temperature. All the radiation from the lower temperature layers deeper in the shock layer is trapped and does not reach the shock.

From former considerations, one realizes that decreasing $n$ from three will cause the flux to become optically thick at smaller values of $\tau_i$ and that increasing the ionization edge will in general lower the value of the flux at a given $\tau_i$ and cause the radiative flux to become optically thick at smaller values of $\tau_i$.

### 4. Application of Results

The previous results were calculated on the basis of a one-level atom. The radiative flux from a two-level hydrogen gas will be calculated in this section by super-position to illustrate how the one-level results can be applied to more complex atoms. Table 1 gives values of the first two ionization edges and their relative optical thicknesses. The quantity $\tau_1\nu_1^3$/

**Table 1 Position of ionization edges and relative optical thickness for atomic hydrogen**

| | Temperature, °K | | | |
|---|---|---|---|---|
| | 10,000 | 15,000 | 20,000 | 25,000 |
| $\bar{\nu}_o$ = | 15.78 | 10.52 | 7.89 | 6.31 |
| $\bar{\nu}_1$ = | 3.94 | 2.63 | 1.97 | 1.58 |
| $\tau_1/\tau_o$ = | $0.581(10)^{-4}$ | $0.300(10)^{-2}$ | $0.216(10)^{-1}$ | $0.704(10)^{-1}$ |
| $\frac{\tau_1}{\tau_o}\left(\frac{\nu_1}{\nu_o}\right)^3$ = | $0.91(10)^{-5}$ | $0.47(10)^{-4}$ | $0.34(10)^{-3}$ | $0.11(10)^{-2}$ |

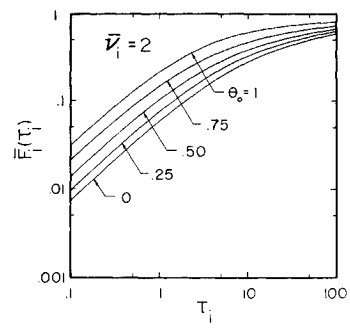


**Fig. 8 Precursor flux; $\bar{F}$ ($\tau_i$) vs $\tau_i$ for several values of $\theta_o$ with $n = 3$.**

($\tau_0\nu_0^3$) in Table 1 is the ratio of the first excited state absorption coefficient to the ground state absorption coefficient evaluated at $\bar{\nu}_o$. Because the absorption coefficient ratio is small and $\bar{\nu}_o - \bar{\nu}_1$ is relatively large, the use of superposition technique appears to be justifiable. Inspection of Table 1 reveals that the accuracy of superposition increases as the temperature decreases.

Figure 9 shows the results obtained by the method of superposition, considering the ground and first excited state of atomic hydrogen at 15,000° and 25,000°K for $\theta_o = 0.5$ as a function of the excited state optical thickness ($\tau_1$).

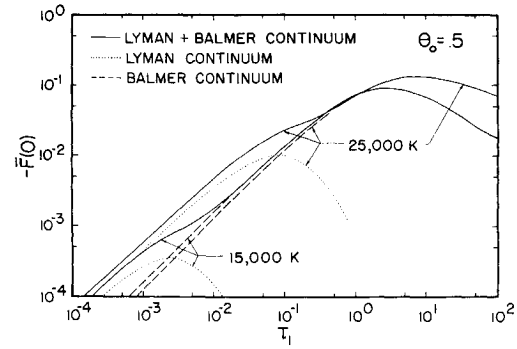


**Fig. 9 Flux from the superposition of the Lyman and Balmer continuum for an atomic hydrogen shock layer as a function of $\tau_i$, $n = 3$.**

The ground state flux is larger than the excited state flux in the optically thin limit; however, the excited state flux is not negligible. As the optical thickness increases, the ground state flux reaches its maximum. It then falls off rapidly because of the influence of the temperature profile and self-absorption and becomes negligible with respect to the excited state flux. As the optical thickness continues to increase, the excited state flux reaches its maximum and begins to fall off due to the same effects.

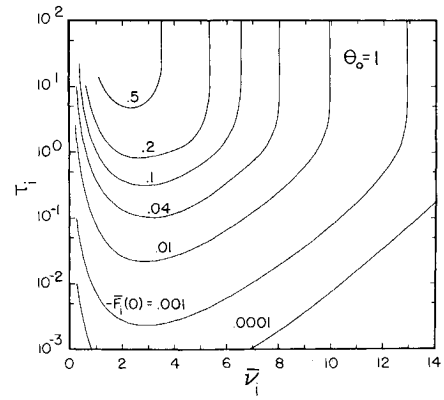


**Fig. 10 Topographical map of $\bar{F}_i$ (0) for isothermal shock layers with $n = 3$.**

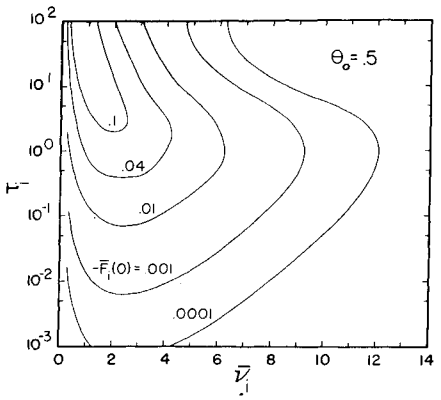


**Fig. 11 Topographical map of $\bar{F}_i$ (0) for nonisothermal shock layers with $n = 3$.**

## IV. Summary and Conclusions

In this study of the continuum radiative flux from nonisothermal stagnation shock layers composed of atomic gases, linear temperature profiles are assumed to exist in the shock layer. This assumption uncouples the radiative transport from fluid mechanics. The Rankine-Hugoniot equations are used to give the temperature just behind the shock wave.

The importance of the ionization edge location and the effect of the spectral shape of the absorption coefficient on the radiation flux are demonstrated through the development of several limiting cases. The method of superposition is used to extend the results to multiple electronic level atomic gases.

The study shows that the location of the ionization edge greatly influences the flux for a given temperature profile and spectral absorption coefficient shape. The spectral shape of the absorption coefficient also influences the flux. These conclusions would also hold for the isothermal case. However, in nonisothermal plasmas, the combined effect of the self-absorption and the temperature profile cause the optically thick limit to be approached from above rather than from below as it does in the isothermal case.

To summarize the results, topographical maps of radiative flux to the body have been drawn as functions of $\tau_i$ and $\bar{\nu}_i$. Figure 10 shows the topographical map for the isothermal case. Figure 11 shows the map for $\theta_o = 0.5$ and Fig. 12 for $\theta_o = 0$. The flux as a function of optical thickness appears on these figures as a line of constant $\bar{\nu}_i$; whereas, the flux as a function of ionization edge location is given by a line of constant $\tau_i$. In the optically thick limit, lines of constant flux become straight lines at a constant value of $\bar{\nu}_i$. For the isothermal case, the flux first increases due to emission and then decreases due to self-absorption when one increases $\bar{\nu}_i$ at a constant value of the optical thickness. When one increases $\tau_i$ at constant $\bar{\nu}_i$, the flux increases toward its optically thick limit. In the nonisothermal plasma, one crosses peaks in the flux as one moves at constant $\tau_i$ and also as one moves at constant $\bar{\nu}_i$; consequently, the flux in the optically thick limit is less than the maximum flux. This is due to the coupling of nonconstant temperature profiles and self-absorption.

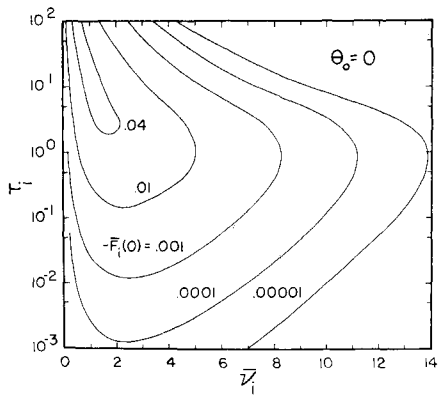


**Fig. 12 Topographical map of $\bar{F}_i$ (0) for nonisothermal shock layers with $n = 3$.**

## References


[1] Goulard, R., Boughner, R. E., Burns, R. K., and Nelson, H. F., "Radiating Flows During Entry into Planetary Atmospheres," IAF Paper RE 70, Oct. 1968, International Astronautical Federation.

[2] Anderson, J. D., "An Engineering Survey of Radiating Shock Layers," *AIAA Journal*, Vol. 7, No. 9, Sept. 1969, pp. 1665–1675.

[3] Nelson, H. F. and Goulard, R., "Equilibrium Radiation from Isothermal Hydrogen-Helium Plasmas," *Journal of Quantitative Spectroscopy and Radiative Transfer*, Vol. 8, No. 6, June 1968, pp. 1351–1372.

[4] Wilson, K. H. and Grief, R., "Radiation Transport in Atomic Plasmas," *Journal of Quantitative Spectroscopy and Radiative Transfer*, Vol. 8, No. 4, April 1968, pp. 1061–1086.

[5] Stickford, G. H. and Menard, W. A., "Bow Shock Composition and Radiation Intensity Calculations for a Ballistic Entry into the Jovian Atmosphere," AIAA Paper 68-787, Los Angeles, Calif., 1968.

[6] Tauber, M. E., "Atmospheric Entry into Jupiter," *Journal of Spacecraft and Rockets*, Vol. 6, No. 10, Oct. 1969, pp. 1103–1109.

[7] Page, W. A., Compton, D. L., Boruski, W. J., Ciffone, D. L., and Cooper, O. M., "Radiative Transport in Inviscid Nonadiabatic Stagnation-Region Shock Layers," AIAA Paper 68-784, 1968; also Goulard, R., ed., "Radiative Gas Dynamics," *AIAA Selected Reprint Series*, Vol. 7, pp. 51–65.

[8] Chin, J. H., "Radiation Transport for Stagnation Flows Including Effects of Lines and Ablation Layers," *AIAA Journal*, Vol. 7, No. 7, July 1969, pp. 1310–1318.

[9] Anderson, J. D., Jr., "Stagnation Point Heat Transfer from a Viscous Nongray Radiating Shock Layer Including the Applicability of Step Model Absorption Coefficients and Sensitivity to Uncertainties in Transport Properties," NOLTR 67, 189, Nov. 1967, U. S. Naval Ordnance Lab., Silver Spring, Md.

[10] Mandell, D. A., "Conduction, Convection, and Radiation in a Nonisothermal Hydrogen Plasma," *Journal of Quantitative Spectroscopy and Radiative Transfer*, Vol. 9, No. 11, Nov. 1969, pp. 1553–1562.

[11] Mandell, D. A., "Radiation Heat Transfer in a Nonisothermal Hydrogen Plasma," Ph.D. dissertation, July 1968, State Univ. of New York at Stony Brook.

[12] Mandell, D. A. and Cess, R. D., "Radiative Transport Quantities for a Hydrogen Plasma," *Journal of Quantitative Spectroscopy and Radiative Transfer*, Vol. 9, No. 7, July 1969, pp. 981-994.

[13] Crosbie, A. L. and Viskanta, R., "The Exact Solution to a Simple Nongray Radiative Transfer Problem," *Journal of Quantitative Spectroscopy and Radiative Transfer*, Vol. 9, No. 5, May 1969, pp. 553–568.

[14] Zeldovich, Ya. B. and Raizer, Yu. P., *Physics of Shock Waves and High Temperature Phenomena*, Academic Press, New York, 1966, pp. 265.

[15] Nikolayev, V. M. and Plastinin, Yu. A., "Studies in Physical Gas Dynamics," edited by A. S. Predvoditelev; also TT F-505, 1968, pp. 35–41, NASA.

[16] Thomas, G. M. and Helliwell, T. M., "Photoionization Cross Sections of Nitrogen, Oxygen, Carbon, and Argon for the Slate-Klein-Brueckner Potential," *Journal of Quantitative Spectroscopy and Radiative Transfer*, Vol. 10, No. 5, May 1970, pp. 423–448.